Appearance Manifolds for Modeling Time-Variant Appearance of Materials

Jiaping Wang* Xin Tong† Stephen Lin† Minghao Pan‡ Chao Wang§ Hujun Bao‡ Baining Guo† Heung-Yeung Shum†

*ICTCAS & GSCAS †Microsoft Research Asia ‡Zhejiang University §Tsinghua University

Figure 1: Synthesis of time-variant weathered appearance from the spatially variant BRDFs of a rusted iron sample (left) measured at a single instant in time. A 3D gargoyle model is rendered at different points in time.

Abstract

We present a visual simulation technique called *appearance manifolds* for modeling the time-variant surface appearance of a material from data captured at a single instant in time. In modeling time-variant appearance, our method takes advantage of the key observation that concurrent variations in appearance over a surface represent different degrees of weathering. By reorganizing these various appearances in a manner that reveals their relative order with respect to weathering degree, our method infers spatial and temporal appearance properties of the material's weathering process that can be used to convincingly generate its weathered appearance at different points in time. Results with natural non-linear reflectance variations are demonstrated in applications such as visual simulation of weathering on 3D models, increasing and decreasing the weathering of real objects, and material transfer with weathering effects.

Keywords: time-variant material model, BRDF, texture synthesis

1 Introduction

Materials in the real world exhibit spatial variations that arise naturally over the course of time. From weathering and wear, a surface undergoes gradual transformations in appearance that progress non-uniformly over the material due to a number of physical factors. Large scale variations in material appearance are mainly influenced by global factors such as object geometry and weathering environment, while small scale characteristics of a material are primarily determined by local factors such as physical material interactions with weather. The local variations in weathered appearance are often intrinsic to the material, a natural characteristic of how it looks. In this work, we address the problem of how to generate convincing weathered appearance of a material on a 3D model over a period of time.

One approach for generating time-variant material appearance is to visually simulate the effects of physical processes, referred to broadly as weathering in this work, on a 3D model (e.g., [Miller 1994; Hsu and Wong 1995; Wong et al. 1997; Chen et al. 2005]). Existing visual simulation techniques can successfully generate large scale variations of material appearance based on global factors such as object geometry and weathering environment. However, these techniques are limited in their ability to produce local characteristics that are intrinsic to a material. In [Chen et al. 2005], local appearance is generated by linearly blending two texture images of the material according to the degree of weathering at each point. Unfortunately, linear blending has two problems. First, the progression of weathered appearance generally follows a non-linear trajectory, and deviations from this trajectory can lead to unnatural appearances of the material. Second, for weathering effects involving texture patterns, intermediate texture variations are ignored.

An alternative approach is to simulate the weathering interactions of a material based on physical principles (e.g., [Dorsey and Hanrahan 1996; Dorsey et al. 1999]). While realistic results have been produced through such simulations, they require substantial computation, and for each new material a complete understanding of its physical weathering process needs to be developed. Another way to obtain physically accurate appearance is to capture a video of a material over time to obtain real-life information on how appearance changes as weathering progresses (e.g., [Georghiades et al. 2005]). Such data-intensive techniques are often challenging in practice because of the need for considerable labor and time. Moreover, technical difficulties with image registration and data storage arise when recording time-variant BRDFs in addition to surface colors.

For realistic and easy modeling of weathered appearance of materials, we present a visual simulation technique that acquires time-

*This work was done while Jiaping Wang was a visiting student at Microsoft Research Asia from the Institute of Computing Technology, Chinese Academy of Sciences (ICTCAS), Graduate School of the Chinese Academy of Sciences (GSCAS).

†Email:{xtong,stevelin,bainguo,hshum}@microsoft.com

variant appearance information from data captured at a single instant in time. Our method capitalizes on the key observation that at a given instant, spatial variations in surface appearance on a weathered material sample correspond to varying degrees of weathering. We utilize these appearance variations to construct an *appearance manifold* that approximates an underlying subspace of weathered surface point appearances for the material. Since the principal mode of variation in the appearance manifold is caused by the progression of weathering, our method infers from the path of this variation the relative degrees of weathering among these surface point appearances. From the assignment of weathering degrees to corresponding appearance states, we can determine spatial and temporal characteristics of the material's weathered appearance, including local appearance properties and valid progressions of surface point appearance over time.

Our method utilizes these time-variant appearance characteristics to generate convincing weathered appearances of the material sample at different points in time. With this evolving material appearance and an object whose time-variant global weathering degree distribution has been determined by existing visual simulation techniques, we propose a new texture synthesis algorithm to generate a time-variant appearance sequence for the given material and object. Although our technique does not perform a physically-based weathering simulation, it can easily synthesize natural-looking non-linear progressions of weathered appearance and its spatial variations, as shown in Fig. 1. Appearance manifolds can also be applied for increasing or decreasing the weathering on a real object. Another application is the transfer of weathered material from one object to another, resulting in a material transformation with realistic weathering detail.

The fact that the appearance manifold is constructed from data captured at a single instant in time makes our technique versatile and easy to use. Indeed, we can even generate time-variant weathering appearance from a single color image for a weathering effect that mainly alters color features. In our experimental results, we also illustrate weathering and deweathering of an object in a single image.

2 Related Work

Weathering Simulation High levels of realism in weathering can be attained through simulations based on physical processes. Several such techniques target material-specific effects, such as metallic patinas [Dorsey and Hanrahan 1996], stone erosion [Dorsey et al. 1999], and paint cracking and peeling [Paquette et al. 2002]. Others have been designed instead for particular forms of weathering, such as water flow [Dorsey et al. 1996], corrosion [Merillou et al. 2001], scratches [Bosch et al. 2004], and lichen growth [Desbenoit et al. 2004]. Specific reflectance models have also been developed for dusty [Blinn 1982] and wet [Jensen et al. 1999; Nakamae et al. 1990] surfaces. These works target high physical accuracy with specialized formulations and considerable computation. In contrast, our approach aims for simplicity in model generation with visually convincing, though not physically precise, synthesis results.

Another approach to generating time-variant surface appearance is to account for the geometric accessibility of surface areas in determining their relative exposure to external effects [Miller 1994; Hsu and Wong 1995; Wong et al. 1997; Chen et al. 2005]. These techniques mainly focus on computing weathering degrees over a surface and pay little attention to the problem of how to determine the actual appearance of a point once its weathering degree is known. Our work on appearance manifolds is complementary to these methods that determine large-scale weathering distributions on an object, and can be used to significantly elevate the quality of local appearance in these techniques.

Recently, methods based on captured time-series data have been presented for modeling appearance variations. An image sequence acquired from a fixed viewpoint has been used to model object appearance over the course of a drying process [Lu et al. 2005] and with respect to changes in certain geometric parameters [Georghiades et al. 2005]. To incorporate view-dependent appearance effects in synthesis, [Lu et al. 2005] adds to the captured diffuse model a decaying specular reflection component that is a function of wetness. In [Gu et al. 2006], a full spatially-varying BRDF is acquired over time, and is factorized into temporal and spatial components to facilitate editing of this time-varying SVBRDF. These works based on appearance histories benefit from an abundance of actual appearance data for modeling. In our method, we also utilize image data but wish to minimize practical difficulties in data acquisition by utilizing a relatively small, easily captured set of data to its full potential.

Texture Synthesis Natural surface variations may also be simulated through texture synthesis. Badler and Becket [Badler and Becket 1990] proposed a system to generate blemish textures based on fractal subdivision techniques. Procedural [Cook 1984; Musgrave et al. 1994] and reaction-diffusion [Turk 1991; Witkin and Kass 1991] texturing methods incorporate randomness in pattern generation to produce a natural-looking solution. However, significant manual intervention is needed to generate a consistent texture sequence that matches natural phenomena.

A data driven texture model was proposed in [Matusik et al. 2005] to generate new color textures by navigating within a subspace induced by a large set of input texture samples. This model could potentially be used to help a user in designing static blemish textures from samples. To generate a consistent texture sequence for an entire weathering process, however, the user would need to carefully select an appropriate set of input samples and precisely guide the navigation among them.

Many example-based texture synthesis approaches as reviewed in [Lefebvre and Hoppe 2005; Kwatra et al. 2005] have been developed to generate texture from input texture samples. Most of these approaches are designed to synthesize static textures. Time-variant textures are synthesized in [Enrique et al. 2005] from small time-variant texture samples. Generally in these techniques, the input texture sample and the synthesized result must be of the same dimension; they cannot be applied in our application where the input is a single 6D SVBRDF while the synthesis output is a 7D time-variant SVBRDF. Recently, a texture optimization approach [Kwatra et al. 2005] was proposed to generate consistent 3D texture sequences controlled by flow fields specified on 2D input textures. However, it handles only homogeneous textures, whereas a time-variant appearance sequence typically exhibits spatial and temporal variations in appearance characteristics. To address progressive variations, a pixel-based approach [Zhang et al. 2003] was proposed to faithfully synthesize texture and its variations on a surface. However, only static textures are generated in their method. For synthesis based on appearance manifold information, we extend the existing texture synthesis methods to obtain consistent texture sequences in which the texture pattern progressively changes both temporally and spatially.

3 Overview

An overview of our system is illustrated in Fig. 2. From spatially variant BRDF data captured from a weathered material sample at a single instant in time, the appearance variations on the sample are analyzed to obtain spatial and temporal appearance properties useful for synthesis of weathering effects.

In this analysis, the course of weathering is assumed to produce gradual monotonic transformations in appearance that exist at spa-

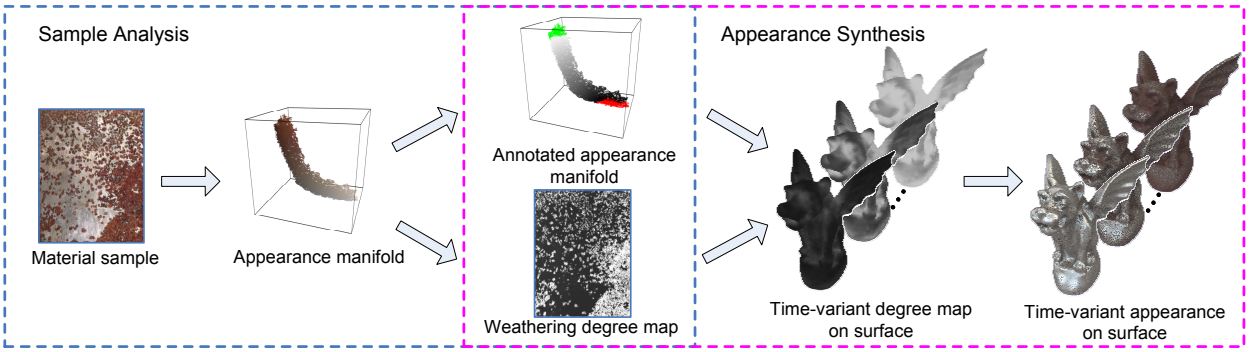

Figure 2: Overview of the appearance manifold technique. In sample analysis, we construct an appearance manifold from material data captured at a single point in time, and with some simple user annotation, we infer the weathering degrees of each appearance state and their spatial distribution. Appearance synthesis uses the information from sample analysis and an input time-variant degree distribution to generate time-variant weathered appearance on a surface. For clarity, the 7D appearance space of reflectance attributes is shown here and in the remainder of the paper in 3D (reduced from 7D by PCA).

tially varying degrees over the surface of the material sample, such that the various states of per-pixel appearance form a manifold in an appearance space. Typically this manifold exhibits a non-linear structure. To obtain a good approximation of this underlying manifold, we plot the captured BRDF data of each surface point in an appearance space defined by reflectance features, and construct a neighborhood graph among these sample points, which we call an *appearance manifold*. With some minor annotation by the user, our method infers from the relative positions of points on the manifold their relative degrees of weathering.

From the association of weathering degrees to appearance states, two characteristics of the material's time-variant appearance can be derived. Since weathering degrees should be non-decreasing over time, the determination of weathering degrees indicates valid temporal progressions in the appearance of a surface point. Also, by assigning these weathering degrees to points on the material sample, we obtain a *weathering degree map* that characterizes local distributions of weathering degree variations for the given material and weathering process.

With this analysis of the material sample, its weathered appearance characteristics can be synthesized onto 3D models. The large-scale temporal progression and spatial distribution of weathering degrees on the model is first obtained from existing visual simulation techniques or user specification. According to these time-variant constraints, corresponding appearance variation details are synthesized onto the surface using the appearance manifold and weathering degree map.

4 Sample Analysis

With data captured from a weathered material sample, we form an appearance manifold by constructing the neighborhood graph for the BRDFs of surface points. From the appearance manifold, we deduce the relative weathering degrees of the various per-pixel appearance states, and hence the valid temporal sequences of pixel appearance. With this degree information, we also form a degree map that represents spatial variations in weathering degree that are present on the sample.

4.1 Appearance Manifolds

In constructing the neighborhood graph of a given material sample $I(x,y)$, we organize the n-dimensional appearance attributes of each pixel (x,y) into a vector, which is plotted as a point in a corresponding n-dimensional appearance space. In our current implementation, we captured a spatially-variant BRDF from flat material samples using a linear light source device as described in [Gardner et al. 2003]. To the BRDF of each point we fit parameters of the isotropic Ward model [Ward 1992; Gardner et al. 2003], such that a 7D appearance space is formed for the material samples presented in this paper.

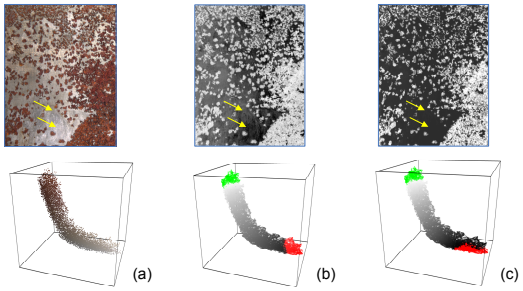

Figure 3: Appearance manifolds constructed from a rusted iron sample. (a) Diffuse image of the material sample, and the initial manifold. (b) Associated weathering degrees determined using Isomap reduction to 1D, exhibited in both the appearance manifold and the degree map. Two unweathered points (indicated by arrows) with different BRDFs are mistakenly assigned to different weathering degrees. (c) With user input, our technique assigns the same weathering degree to these two points. The red (green) set in (b) and (c) indicates the least (most) weathered points.

Since sample points in the appearance space typically form a dense distribution as exemplified in Fig. 3(a), we utilize the ε-rule and k-rule [Tenenbaum et al. 2000] to construct the neighborhood graph. Specifically, an initial graph is formed using the k-rule, which connects each point to its k nearest neighbors ($k = 8$ for all examples in this paper). Outliers in the graph are then pruned using the ε-rule, which allows connections only between points separated by a distance less than a threshold ε. In our implementation, we set $\varepsilon = 1.5d_p$ where d_p is the average pairwise distance between connected points after applying the k-rule. To compute d_p, we first construct an appearance vector for each of the two points by sampling its BRDF over a set of lighting and viewing directions. The distance of the two samples is then computed as described in [Matusik et al. 2003] by the L^2 distance of their appearance vectors in a logarithm space.

From the structure of the resulting neighborhood graph, our

method infers an ordering of points with respect to weathering degree. One possible approach is to perform dimensionality reduction [Tenenbaum et al. 2000; Roweis and Saul 2000] to map the data into a 1D curve that indicates relative degrees of weathering. However, this mapping may be influenced by secondary appearance variations, such as from material non-uniformity and incidental weathering processes, that are non-orthogonal to the principal mode of weathering variation. Consequently, weathering degrees might not be reliably determined in this manner. For example, although the two points indicated in Fig. 3(b) exhibit no weathering, their appearance variations lead to different estimates of weathering degree by dimensionality reduction.

To approximately factor out the effects of non-orthogonal secondary variations from weathering degrees, we take advantage of user interaction to incorporate high-level knowledge into the analysis process. Specifically, the user assists our technique in identifying the sets of most weathered and least weathered points in the appearance manifold. The user is prompted to highlight pixels in $I(x,y)$ to form initial sets X_0', X_1' of least and most weathered points. The set X_1' is then dilated according to

$$X_1 = \{\, x_i \mid \phi(x_i, x_0') \;>\; \lambda\, \Phi(X_0', X_1') \,\},$$

where the appearance distance $\phi(x_i, x_j)$ between points x_i and x_j is defined as their geodesic distance in the manifold (e.g., the shortest path along the connected nodes between x_i and x_j), $\Phi(X_0', X_1')$ denotes the minimum appearance distance between X_0' and X_1', x_0' denotes the closest point in X_0 to x_i, and λ is a parameter set to 0.9 in our implementation. X_1 is then made convex by including all points that lie on geodesics between pairs of its points. A set X_0 of least weathered points is determined similarly.

Between these two sets, a gradual transition in appearance exists from least weathered to most weathered. According to the relative distances of a point x from the two sets, we define its degree of weathering as a scalar function of appearance:

$$\varphi(x) = \frac{\phi(x, x_0')}{\phi(x, x_0') + \phi(x, x_1')}$$

where x_0' and x_1' are respectively the closest points in X_0 and X_1 to x. For all samples captured in our experiments, this approach produces more accurate weathering degrees. As exhibited in Fig. 3(c), the same weathering degree is correctly determined for the two indicated points using our approach. For a weathering process that leads to complex appearance manifolds with significant twist and turns, a greater amount of user input may be needed to separate weathering variations from appearance variations unrelated to weathering.

With the assignment of degree values to points in the appearance manifold, we can determine valid sequences of weathered appearance for a surface point. Since weathering degrees naturally increase over time, the appearance of a point must follow a forward path from a point x_0 to x_n that satisfies $\phi(x_{i+1}) \geq \phi(x_i)$ for all neighboring pairs of points x_i, x_{i+1} on the path. Our technique utilizes validity of appearance sequences as a constraint in weathered appearance synthesis. To generate a valid appearance sequence between two points x_0, x_n, a straightforward way is simply to interpolate along the shortest path between them.

A manifold model of measured BRDFs was also constructed in [Matusik et al. 2003], which employs non-linear dimensionality reduction to determine a low-dimensional characterization of high-dimensional BRDF data sets. In our method, with the knowledge that the primary variation of captured BRDFs from a material is caused by weathering, we focus instead on deriving the non-linear changes in the BRDFs of a given material with respect to weathering degree. Additionally, spatially-variant BRDFs and their temporal variations are handled in our approach.

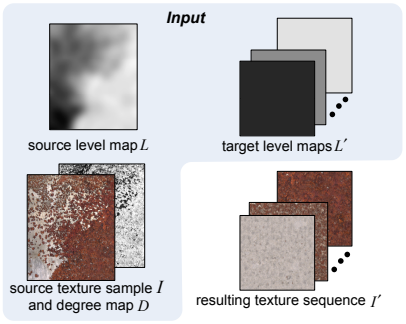

Figure 4: Overview of appearance synthesis. The input consists of a sample texture I, its associated degree map D, its level map L, and sequence of target weathering level maps L'. The result is a time-variant appearance sequence I'.

4.2 Weathering Degree Maps

By replacing appearance values of the sample with degree values, we obtain a weathering degree map as shown at the top of Fig. 3(c), which displays spatial variations in weathering degree over the material sample. Although the global distribution of weathering degrees in the degree map tends to be specific to the shape of the material sample, for many materials the local variations are an intrinsic characteristic of its weathered appearance. These textures of weathering degree often change over the course of time. As exemplified in Fig. 3(a), neighborhoods at different levels of weathering may exhibit different spatial patterns, while local areas that have similar weathering levels have textures that approximately follow the same stationary stochastic model. In the following appearance synthesis process, we account for these time-variant local weathering characteristics of the material sample.

5 Appearance Synthesis

With the appearance manifold and computed degree map of a material sample, our method synthesizes detailed weathering appearance onto a 3D model according to a given large scale time-variant distribution of weathering degrees over the surface. This degree distribution can be generated using existing visual simulation techniques or by manual specification.

To generate local weathering appearance on a 3D model labeled with only large-scale degree variations, we identify pixels on the model and on the material sample that have a similar local level of weathering, computed by averaging the weathering degrees within $2N \times 2N$ local neighborhoods in their corresponding degree maps, where N is largest neighborhood size used in the texture synthesis procedure. These average degree values are stored in structures called weathering level maps. Local weathering appearance is then synthesized onto the model in a manner consistent with weathering level. The resulting appearance sequence should also adhere to two temporal constraints. First, the time-variant appearance sequence for each pixel $p = (x,y)$ should follow a valid path in the appearance manifold. Second, the spatial characteristics of appearance should change smoothly over time.

A naive approach to appearance synthesis is to generate each frame independently. However, generated appearance sequences would exhibit flickering due to a lack of frame-to-frame coherence. Another possible solution is to synthesize the first frame on the surface and then extrapolate the appearance of each point along the appearance manifold. Although this approach could generate a consistent time sequence for each surface point, a convincing evolution of texture patterns is unlikely to be obtained. The artifacts gener-

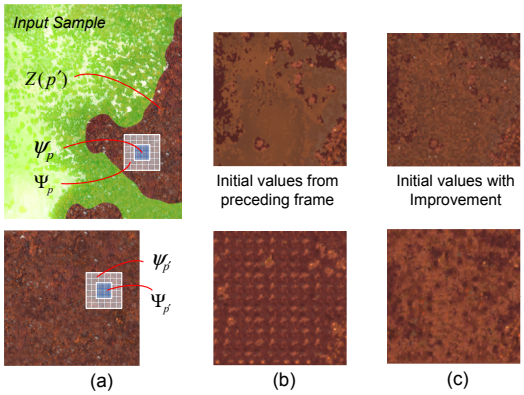

Figure 5: Appearance synthesis for each frame. (a) Synthesis configuration. The unmasked (brown) region on the input sample texture (top) contains the set $Z(p')$ of candidates for p' in a synthesized frame (bottom). (b) Initial values extrapolated from the preceding frame (top), and the resulting synthesis result (bottom), which contains undesirable repetition of texture patterns. (c) Improvement of initial values by considering neighborhood information on the sample (top), and the resulting synthesis result (bottom).

ated by these two straightforward approaches are exemplified in the supplemental video.

In this paper, we propose a multi-scale texture synthesis technique to generate a time-variant appearance sequence from input samples. For simplicity, we describe only our synthesis algorithm for an image appearance sequence, which can then be easily modified to synthesize a time-variant appearance sequence on a surface. As illustrated in Fig. 4, for a given input sample texture $I(p)$, its associated degree map $D(p)$, and its level map $L(p)$, we synthesize a time-variant appearance sequence $I'(p',t_i)$, $i = 0,1,2..,n$, whose local textures are consistent with the sequence of weathering level maps $L'(p',t_i)$ computed from the given large-scale time-variant degree distribution.

In our algorithm, the appearance sequence is synthesized frame by frame. For each frame, the synthesis is executed in three steps. We first initialize the appearance of each frame from the appearance of the preceding frame. Specifically, we initialize the degree values of each frame by extrapolating those of the preceding frame according to $D'(p',t_i) = D'(p',t_{i-1}) + L'(p',t_i) - L'(p',t_{i-1})$ for each pixel p' in the frame. To determine an initial appearance for the frame, we then interpolate according to these initial degree values along the shortest path in the appearance manifold between points for $I'(p',t_{i-1})$ and the set X_1 of most weathered points. Although this initialization produces valid temporal sequences of weathered appearance for each pixel, it does not account for progressive texture variations from frame to frame. Without these progressive changes in local degree distributions, the quality of matches in the synthesis process becomes poor, and this may result in a repetition of texture patterns as illustrated in Fig. 5(b).

To avoid this problem, we incorporate the information from input samples to obtain an improved initialization in the second step. As illustrated in Fig. 5(a), let Ψ_p and ψ_p respectively represent an $N \times N$ neighborhood and an $m \times m$ sub-neighborhood centered on p, where $m = N/3$ in our implementation. We divide the frame into a set of $m \times m$ patches, and we denote as P' the centers of all these non-overlapping patches. For each $p' \in P'$, we average the appearance values in neighborhood $\psi_{p'}$ with those in ψ_p of a randomly selected pixel p from a candidate set

$$Z(p') = \{p : |L(p) - L'(p',t_i)| \leq \kappa\},$$

where $\kappa = 0.15$ in our implementation. With this approach, changes in texture characteristics over time can effectively be incorporated. For the first frame in the sequence, which cannot be extrapolated from others, we initialize its values $I'(p',t_0)$ and $D'(p',t_0)$ based on random patches ψ_p from candidate sets $Z(p')$.

Finally, the initial appearance frame is refined by synthesis with multiple neighborhood scales. For each scale, our algorithm traverses all pixels in P' and synthesizes an $m \times m$ patch for each pixel. Specifically, for each $p' \in P'$, we construct its candidate set $Z(p')$ and then search for the pixel p in I whose patch Ψ_p best matches $\Psi_{p'}$ in the L^2-norm. For the search result Ψ_p, we copy $q \in \psi_p$ to $q' \in \psi_{p'}$ if it is temporally coherent, i.e., the degree value of q is greater than or equal to that of q' in the preceding frame. Otherwise, the appearance and degree values of q' are kept unchanged. This procedure is repeated for successively smaller sizes of Ψ_p until N is decreased to 3. Fig. 5(c) displays the final synthesis result refined from the improved initial values.

In practice, frame-by-frame synthesis of the appearance sequence is time-consuming and not necessary because of the small changes in appearance and degree between the two adjacent frames. For greater efficiency, we synthesize selected key frames from the sequence and interpolate intermediate frames. With the first frame as a key frame k_0, we select successive key frames according to $\{k_i \mid max_{p'}(L'(p',k_i) - L'(p',k_{i-1})) > \varepsilon\}$, where ε is set to 0.2 in our implementation. The appearance of each pixel in an intermediate frame is interpolated along the shortest path in the appearance manifold between the corresponding pixels in the preceding and subsequent key frames.

6 Other Applications

With the association of weathering degrees to appearance vectors, other weathering applications become easy to formulate. We describe techniques for weathering and deweathering the appearance of a real object, and for material transfer from one object to another with weathering effects.

6.1 Weathering and Deweathering

In weathering and deweathering of an input weathered object, sample analysis is first performed to obtain the object's degree map, which is then used to generate a time-variant degree sequence with some user assistance. To aid the user in this process, we present a tool shown in Fig. 6 for easy editing of a default degree sequence with interactively updated appearance sequences displayed as feedback.

In the default degree sequence, the user can select key frames for degree modification. With the user tool, the degree values d in a key frame can be transformed to new values d' by adjusting a mapping function $d' = f(d)$. Additionally, the tool allows the user to hand-paint degree modifications in a key frame. As the user applies these alterations, the degree values in non-key frames are interpolated among key frames. To efficiently update the appearance sequence after each degree sequence revision, our tool simply warps the appearance sequence of each pixel in correspondence with its change in degree. After the user has fully completed adjusting the degree sequence, the original appearance synthesis procedure is applied again to obtain a more refined appearance sequence.

In our current implementation, the default degree sequence is computed by placing the object's degree map at the center of the sequence and linearly increasing (decreasing) the degree values in weathering (deweathering) frames until all degree values reach 1.0 (0.0). A corresponding default appearance sequence is then computed using the appearance synthesis algorithm in Sec. 5. The input appearance of the object is used as the initial appearance frame from which the rest of the default sequence is synthesized into the future and the past.

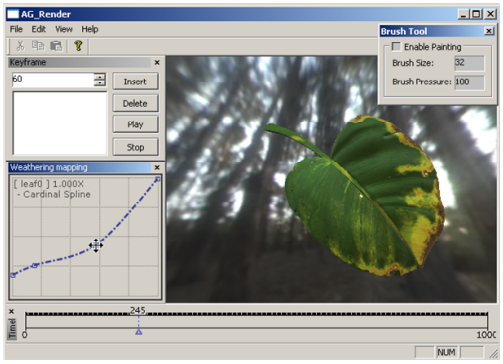

Figure 6: GUI for weathering and deweathering. Degree values are transformed according to a user-adjustable function. Also, modifications of degree values can be specified in the image by hand.

6.2 Weathering Transfer

Another image-based application is to render a weathered object O_1 with a different material of another weathered object O_2. With user assistance, our technique achieves this by performing sample analysis on the two objects to determine their weathering characteristics, and then synthesizing the appearance of O_2 onto O_1 in a manner consistent with O_1's shape-dependent weathering degree distribution. This synthesis proceeds as in the method described in Sec. 5, except that appearance attributes from O_2 are synthesized to the degree map of O_1.

The time-variant appearance of O_1 can also be synthesized with the material of O_2 by extrapolating O_1's degree map into a degree sequence using the techniques presented in Sec. 6.1. With this degree sequence, the appearance manifold and degree map of O_2 can then be used to synthesize an appearance sequence using the method in Sec. 5.

7 Results

We implemented the appearance manifold system on a PC with a Pentium IV 2.8GHZ CPU, 2GB memory, and a Nvidia Geforce7800 256MB graphics card. Sample resolutions and the largest window sizes used in appearance synthesis are given in Table 1 for the presented examples. For computational efficiency, the appearance manifold is constructed using 10,000 sampled pixels with distinct appearance vectors, and the weathering degree values of all other pixels are copied from the nearest sample point in the appearance space. We adapted the algorithm in [Kautz et al. 2000] to render time-variant appearances of objects with global illumination. For the examples in this paper, sample analysis requires approximately five minutes, and appearance synthesis times range from one to five hours. Rendering is performed at about 20 Hz.

Fig. 1 displays a rusting gargoyle rendered with global illumination. The global distribution of the rust and its temporal variations are simulated by γ-ton tracing [Chen et al. 2005]. The characteristics of the local rust patterns on the gargoyle change with time in consistency with the different neighborhoods in the original sample at different weathering levels. In the supplemental video, we also demonstrate with this model the appearance differences between linear texture blending and our non-linear appearance manifold technique. Linear blending is seen to produce appearances that diverge considerably from rusting iron, such as rust colors with significant specularity.

Sample	Rust	Banana	Leaf	Patina	Wood	Stone
Width	269	540	970	1010	640	800
Height	361	499	712	750	480	498
Window size	32	22	5	26	22	32

Table 1: Sample resolutions and largest window sizes for synthesis.

Three bananas at different states of weathering are exhibited in Fig. 7, where their appearances are all synthesized using the material sample shown in (a). In this example, the initial degree map on the rendered bananas is specified by an artist, and then the weathering/deweathering procedure is used to generate the weathering sequence. The appearance of spatial variations and their evolution over time are synthesized onto the new objects to produce convincing results.

Fig. 8(a) shows an image of a leaf sample and its degree map. We demonstrate weathering on only the foremost leaf. The other leaves were designed by an artist using conventional texture mapping. In this example, we also captured the translucency of each point on the sample. Using our weathering and deweathering system, we generate an appearance sequence from the original sample, shown for three time instants in Fig. 8(b-d). In the supplemental video, the translucency of the leaf is seen to vary with greater weathering, while the specularity of the leaf gradually lessens. This sequence was generated based on user specification of six key frames.

Fig. 9 displays a buddha model scanned from a real object with textures generated using the texture montage technique [Zhou et al. 2005]. To compute its weathering degree map shown in the upper-left corner of Fig. 9(a), we analyzed the diffuse color of the buddha under ambient lighting, which clearly reveals variations of tarnish on the surface. Based on this analysis, our method for weathering transfer generates renderings of the buddha in Fig. 9(b-d) that are consistent with the weathering degrees of the original model, but utilizes different weathered materials.

An interesting application of the appearance manifold technique is weathering and deweathering of an object shown in a single image. In this application, we first segment out the object of interest and then perform sample analysis on it. To minimize the effects of intensity variations due to shading, we convert pixel colors into $L\alpha\beta$ space and then use only the $\alpha\beta$ channels for analysis. To each degree value d, we associate the average luminance L_d of all pixels of the same degree. Shading variations in the image are then approximately separated from weathering and stored in a illumination map $L'(x,y) = L(x,y)/L_{d(x,y)}$, where $L(x,y)$ is the original luminance of the pixel and $d(x,y)$ denotes the pixel degree. After generating a new degree map as described in Sec. 5, we obtain the weathered/deweathered color for each pixel by interpolating along the shortest path from its point in the appearance manifold to the most/least weathered point sets. The final result is obtained by multiplying the illumination map with the weathering color image, as displayed in Fig. 10. Non-weathering variations such as from sharp specularities and texture may reduce the performance of this basic method, but could potentially be addressed by further image analysis. Since the input is just a single image, this application targets weathering effects that primarily alter only color appearance features.

8 Discussion and Conclusion

The proposed appearance manifold technique generates weathering sequences that are consistent with the changing local reflectance characteristics of a material over time. It complements existing visual simulation techniques that are designed to compute weathering degree distributions, and leads to various weathering applications for synthetic 3D models, real weathered objects, and even single snapshots of weathered objects. With this method, the input data

is simple to acquire, and natural non-linear appearance variations over time are easy to produce.

Since reorganization of appearance data into an appearance manifold determines only a sequential relationship among the observed weathered appearances, rather than correspondences to actual degrees of weathering, the simulations of weathering effects are not physically precise. The intent of our method, however, is to generate visually compelling weathered appearance from a small amount of easily captured image data.

To effectively analyze a material sample with this technique, the underlying weathering process should produce smooth temporal variations in appearance. In cases where weathering produces sharp changes in reflectance or significantly alters surface geometry, such as from cracking or peeling, the resulting discontinuities in the appearance manifold may impair the inference of weathering degrees. Since weathering degrees are assigned with respect to a primary mode of appearance variation, our method also cannot handle variations caused by multiple weathering effects, or materials with significant intrinsic variations.

Although input data from only a single material sample and time instant is needed, appearance manifold analysis can also jointly handle data from multiple samples and instants in time, as long as the data all represents the same weathering process of the same material. Without the need for surface point correspondences, BRDFs can be recorded at different times without image registration. This property is particularly useful in broadening the range of modeled weathering effects. For example, sample analysis for the banana in Fig. 7 was performed using two bananas at different stages of ripening.

In the future, we plan to extend appearance manifolds to include additional forms of weathering effects. Through an analysis of captured BTF data, local geometry variations from weathering may potentially be incorporated into our weathering appearance framework. In addition, identifying and modeling multiple types of weathering that jointly alter the appearance of a material is an interesting direction for investigation. Aside from expanding the modeling capabilities of our system, we also intend to examine ways to accelerate rendering of time-variant appearance.

Acknowledgements

The scenes in Fig. 7 and Fig. 8 were modeled by Rui Jin and Yuan Tian. The grille image in Fig. 10 was copied from MaYang's texture library (http://www.mayang.com/textures). The authors thank Kun Zhou and Dong Xu for discussions on manifold learning, and the anonymous reviewers for their helpful suggestions and comments. Minghao Pan and Hujun Bao were supported in part by The National Basic Research Program of China (973 Program) under Grant No. 2002CB312102, the Natural Science Foundation of China under Grant No. 60021201, and The Cultivation Fund of the Key Scientific and Technical Innovation Project, Ministry of Education of China, under Grant No. 705027.

References

BADLER, N. I., AND BECKET, W. 1990. Imperfection for realistic image synthesis. *J. Visualization and Computer Animation 1* (Aug), 26–32.

BLINN, J. F. 1982. Light reflection functions for simulation of clouds and dusty surfaces. In *SIGGRAPH '82*, 21–29.

BOSCH, C., PUEYO, X., MERILLOU, S., AND GHAZANFARPOUR, D. 2004. A physically-based model for rendering realistic scratches. *Computer Graphics Forum 23*, 3, 361–370.

CHEN, Y., XIA, L., WONG, T.-T., TONG, X., BAO, H., GUO, B., AND SHUM, H.-Y. 2005. Visual simulation of weathering by γ-ton tracing. *ACM Trans. Graph. 24*, 3, 1127–1133.

COOK, R. L. 1984. Shade trees. In *SIGGRAPH '84*, 223–231.

DESBENOIT, B., GALIN, E., AND AKKOUCHE, S. 2004. Simulating and modeling lichen growth. *Computer Graphics Forum 23*, 3, 341–350.

DORSEY, J., AND HANRAHAN, P. 1996. Modeling and rendering of metallic patinas. In *SIGGRAPH '96*, 387–396.

DORSEY, J., PEDERSEN, H. K., AND HANRAHAN, P. 1996. Flow and changes in appearance. In *SIGGRAPH '96*, 411–420.

DORSEY, J., EDELMAN, A., JENSEN, H. W., LEGAKIS, J., AND PEDERSEN, H. K. 1999. Modeling and rendering of weathered stone. In *SIGGRAPH '99*, 225–234.

ENRIQUE, S., KOUDELKA, M., BELHUMEUR, P., DORSEY, J., NAYAR, S., AND RAMAMOORTHI, R. 2005. Time-varying textures. Tech. Rep. CUCS-023-05, Columbia University.

GARDNER, A., TCHOU, C., HAWKINS, T., AND DEBEVEC, P. 2003. Linear light source reflectometry. *ACM Trans. Graph. 22*, 3, 749–758.

GEORGHIADES, A. S., LU, J., XU, C., DORSEY, J., AND RUSHMEIER, H. 2005. Observing and transferring material histories. Tech. Rep. 1329, Yale University.

GU, J., TU, C.-I., RAMAMOORTHI, R., BELHUMEUR, P., MATUSIK, W., AND NAYAR, S. 2006. Time-varying surface appearance: Acquisition, modeling and rendering. *ACM Trans. Graph. 25*, 3.

HSU, S.-C., AND WONG, T.-T. 1995. Simulating dust accumulation. *IEEE Comput. Graph. Appl. 15*, 1, 18–22.

JENSEN, H. W., LEGAKIS, J., AND DORSEY, J. 1999. Rendering of wet materials. In *Rendering Techniques 99*, 273–282.

KAUTZ, J., VÁZQUEZ, P.-P., HEIDRICH, W., AND SEIDEL, H.-P. 2000. Unified approach to prefiltered environment maps. In *Rendering Techniques 2000*, 185–196.

KWATRA, V., ESSA, I., BOBICK, A., AND KWATRA, N. 2005. Texture optimization for example-based synthesis. *ACM Trans. Graph. 24*, 3 (July), 795–802.

LEFEBVRE, S., AND HOPPE, H. 2005. Parallel controllable texture synthesis. *ACM Trans. Graph. 24*, 3 (July), 777–786.

LU, J., GEORGHIADES, A. S., DORSEY, J., RUSHMEIER, H., AND XU, C. 2005. Synthesis of material drying history: Phenomenon modeling, transferring and rendering. *Euro. Workshop Nat. Phenomena*.

MATUSIK, W., PFISTER, H., BRAND, M., AND MCMILLAN, L. 2003. A data-driven reflectance model. *ACM Trans. Graph. 22*, 3, 759–769.

MATUSIK, W., ZWICKER, M., AND DURAND, F. 2005. Texture design using a simplicial complex of morphable textures. *ACM Trans. Graph. 24*, 3, 787–794.

MERILLOU, S., DISCHLER, J.-M., AND GHAZANFARPOUR, D. 2001. Corrosion: simulating and rendering. In *Graphics Interface 2001*, 167–174.

MILLER, G. 1994. Efficient algorithms for local and global accessibility shading. In *SIGGRAPH '94*, 319–326.

MUSGRAVE, F. K., PEACHEY, D., PERLIN, K., AND WORLEY, S. 1994. *Texturing and modeling: a procedural approach*. Academic Press Professional, Inc., San Diego, CA, USA.

NAKAMAE, E., KANEDA, K., OKAMOTO, T., AND NISHITA, T. 1990. A lighting model aiming at drive simulators. In *SIGGRAPH '90*, 395–404.

PAQUETTE, E., POULIN, P., AND DRETTAKIS, G. 2002. The simulation of paint cracking and peeling. In *Graphics Interface 2002*, 59–68.

ROWEIS, S., AND SAUL, L. 2000. Nonlinear dimensionality reduction by locally linear embedding. *Science 290*, 5500 (Dec), 2323–2326.

TENENBAUM, J. B., DE SILVA, V., AND LANGFORD, J. C. 2000. A global geometric framework for nonlinear dimensionality reduction. *Science 290*, 5500 (Dec), 2319–2322.

TURK, G. 1991. Generating textures on arbitrary surfaces using reaction-diffusion. In *SIGGRAPH '91*, 289–298.

WARD, G. J. 1992. Measuring and modeling anisotropic reflection. In *SIGGRAPH '92*, 265–272.

WITKIN, A., AND KASS, M. 1991. Reaction-diffusion textures. In *SIGGRAPH '91*, 299–308.

WONG, T.-T., NG, W.-Y., AND HENG, P.-A. 1997. A geometry dependent texture generation framework for simulating surface imperfections. *Euro. Workshop Rendering*, 139–150.

ZHANG, J., ZHOU, K., VELHO, L., GUO, B., AND SHUM, H.-Y. 2003. Synthesis of progressively-variant textures on arbitrary surfaces. *ACM Trans. Graph. 22*, 3 (July), 295–302.

ZHOU, K., WANG, X., TONG, Y., DESBRUN, M., GUO, B., AND SHUM, H.-Y. 2005. Texturemontage: Seamless texturing of arbitrary surfaces from multiple images. *ACM Trans. Graph. 24*, 3, 1148–1155.

Figure 7: Three bananas at different stages of weathering. (a) The original sample and its degree map after analysis. (b)(c)(d) Rendering results of bananas under global illumination. The most weathered banana at the bottom is kept constant for reference.

Figure 8: A leaf at different stages of weathering. The weathering process is simulated by our weathering and deweathering process. (a) The original sample and its degree map after analysis. (b) Rendering result of the leaf after deweathering. (c) Rendering result of the leaf after less deweathering. (d) Rendering result of the leaf after weathering.

Figure 9: Rendering results of a Buddha with different material. (a) The original material, with the degree map shown in the upper-left. (b) With transferred brass and patina effects. (c) With transferred stone and weathering effects. (d) With transferred wood and weathering effects.

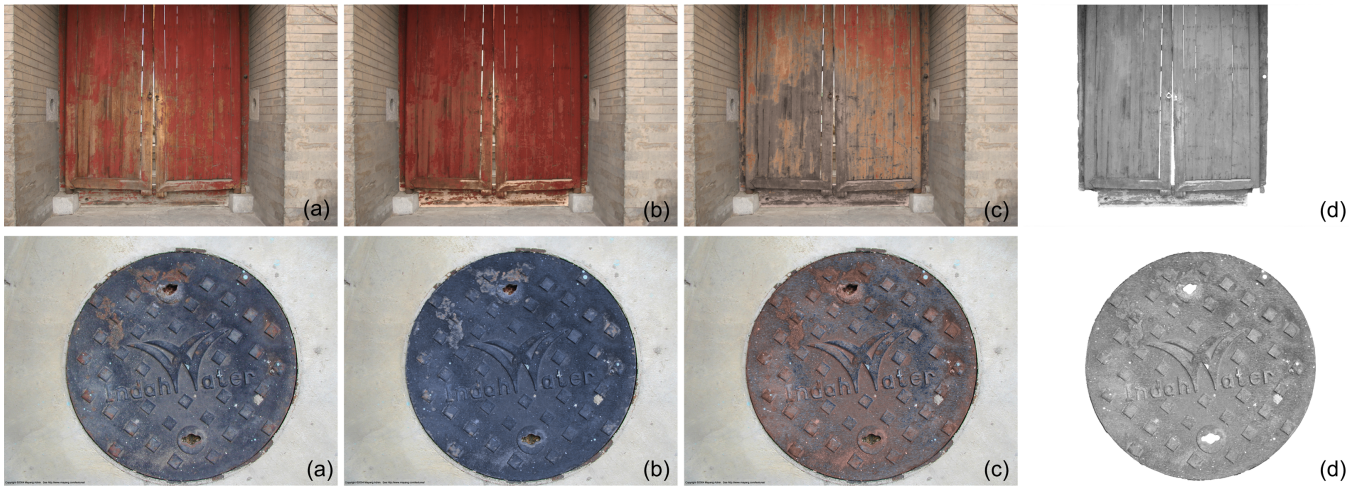

Figure 10: Image weathering and deweathering. (a) Original images. (b) Result of deweathering. (c) Result of weathering. (d) Illumination maps.